# Modeling and Model Validation for Electron Beam Nanometrology


John S. Villarrubia, Kerim T. Arat, Glenn Holland, and András E. Vladár

Microsystems and Nanotechnology Division, Physical Measurement Laboratory, National Institute of Standards and Technology



## Abstract

Nanotechnology applications often require dimensional measurements with very low uncertainties. The scanning electron microscope (SEM) beam scatters by more than this amount, so such uncertainties require accurate model-based signal interpretation. Schematically, $I(x) = M(x;\boldsymbol{p})$ with $I(x)$ the measured signal, $x$ the lateral coordinate, $\boldsymbol{p}$ the vector of sample and instrument parameters, and $M$ the physics-based model function. Unknown parameters in the $\boldsymbol{p}$-vector, including e.g., feature shape and size, are assigned by a best fit criterion.

Models are approximate, there are many of them, and their differences are especially notable at low energies. The associated errors are difficult to estimate. Ideally, measurements would narrow the choice of models, but measured basic quantities like secondary electron yield vary by factors of 2 to 4 among laboratories.

We are constructing a yield measurement instrument to address this problem. It will be inside an ultra-high vacuum chamber with facilities for sample cleaning and characterization. A spherical retarding field analyzer (RFA) will measure secondary and backscattered electron yields and energy spectra as functions of beam energy and angle of incidence. The RFA is designed to have high collection efficiency that is nearly constant with angle.


## Background

To perform a measurement, we interpret the measuring instrument's signal with a simulator with an assumed interaction physics. Our simulator, JMONSEL[1], can represent complex sample shapes.

JMONSEL sample representations:
1. Constructive solid geometry
2. Height maps
3. Tetrahedral mesh

These permit realistic complex shapes.

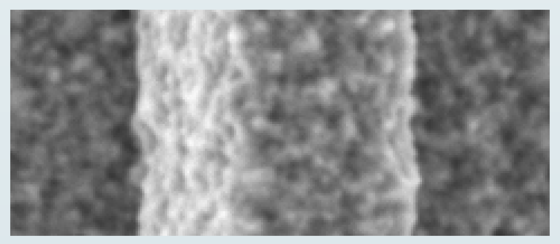

JMONSEL simulation of a line with a prescribed roughness power spectrum

JMONSEL simulation of an intentional defect pattern

Below on the left we see simulated electron trajectories in a FinFET fin/space array. The right is a generic trajectory step.

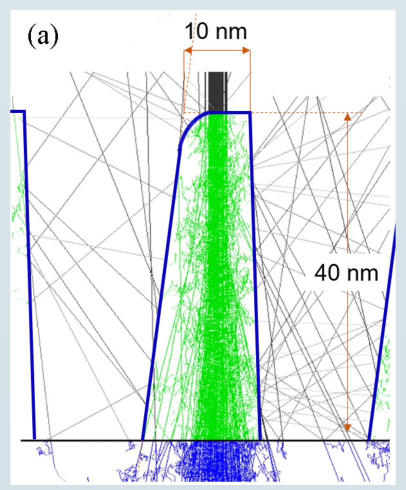


Simulated trajectories

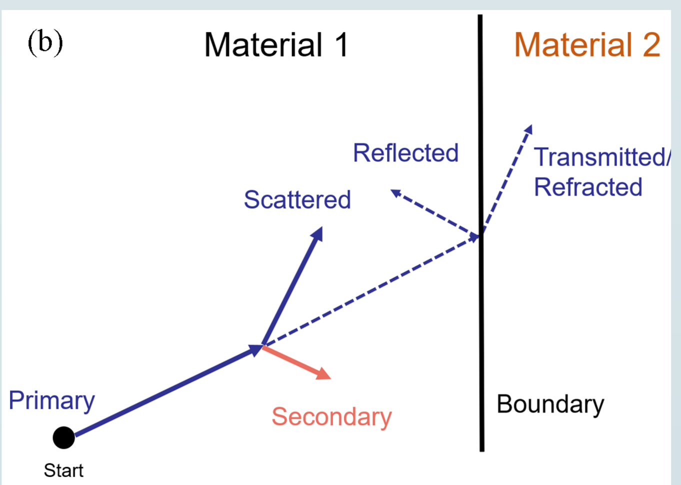


Events that may occur in a trajectory step.

| Event type | How simulated |
|---|---|
| Electron-atom elastic scattering | Mott theory, partial wave analysis, computed by ELSEPA[2] |
| Secondary electron generation | Dielectric function theory, Penn method[3] |
| Electron-optical phonon scattering | Llacer & Garwin[4], following Ganachaud & Mokrani[5] implementation |
| Boundary crossing | Quantum transmission, exponential barrier: $U(x) = \frac{\Delta U}{1+e^{-\frac{2x}{w}}}$ |

Example measurement: (1) The image is measured in an SEM. (2) Sample parameters (fin width, sidewall angles and rounding) are adjusted to produce the best fit (black curve) to the measured profile (red error bars). The shape described by these parameters (blue curve) is the measurement result. The panel on the right overlays such results on a subsequent TEM of the sample.

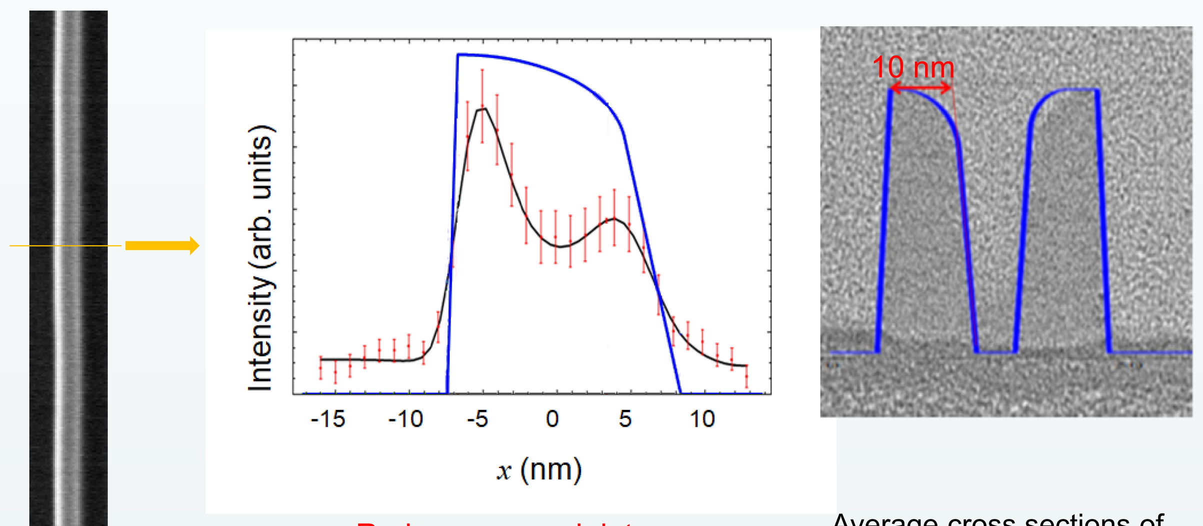


Measured signal

Red = measured data
Black = best fit intensity
Blue = inferred line shape

Average cross sections of the 3-D shape agree well with TEM cross-sections.

## Model Uncertainties

To the extent that our models are approximate, our inferred measured values are also approximate. Potentially important approximations in the models:

1. Elastic scattering: Mott theory is a binary scattering theory. We expect it to break down at low energy (electron λ close to nearest neighbor atomic distance).
2. Inelastic scattering with dielectric function theory:
   a. Omits exchange and correlation or treats it in high-energy approx.
   b. Has different versions depending on zero (Penn[3]) or non-zero (Mermin[6]) plasmon damping
   c. Treats interband transitions as though they are plasmons
   d. Is based on a high-energy 1st Born approximation
   e. Is a theory of energy *loss* by the primary electron; Final energy and momentum of a generated secondary electron require more assumptions regarding its initial state.
3. Inputs for models (e.g., energy loss function, plasmon lifetimes, barrier width…) are uncertain.
4. …

Different models predict different mean free paths:

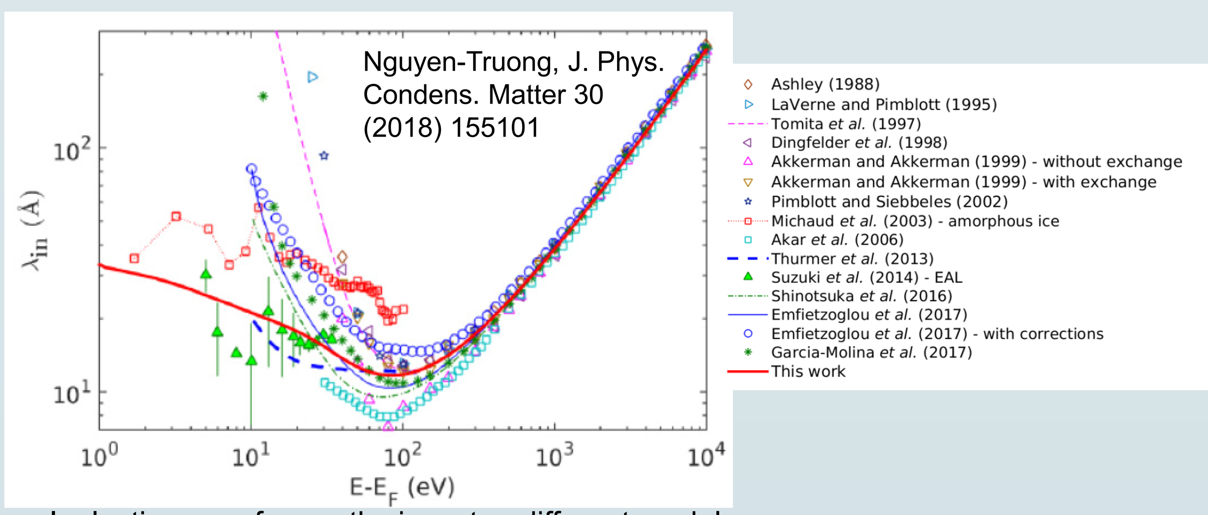


Inelastic mean free paths in water, different models

There is limited measurement data for such small mean free paths, owing partly to the extra complexity of multiple scattering. Yield predictions (yield $= \frac{\text{electrons out}}{\text{electrons in}}$) for secondary (SEY) or backscattered (BSY) are also model-dependent and are in principle measurable. Could yield vs. energy or yield vs. angle of incidence (topographic yield) help us choose among the models?

Secondary electron yield measured values:

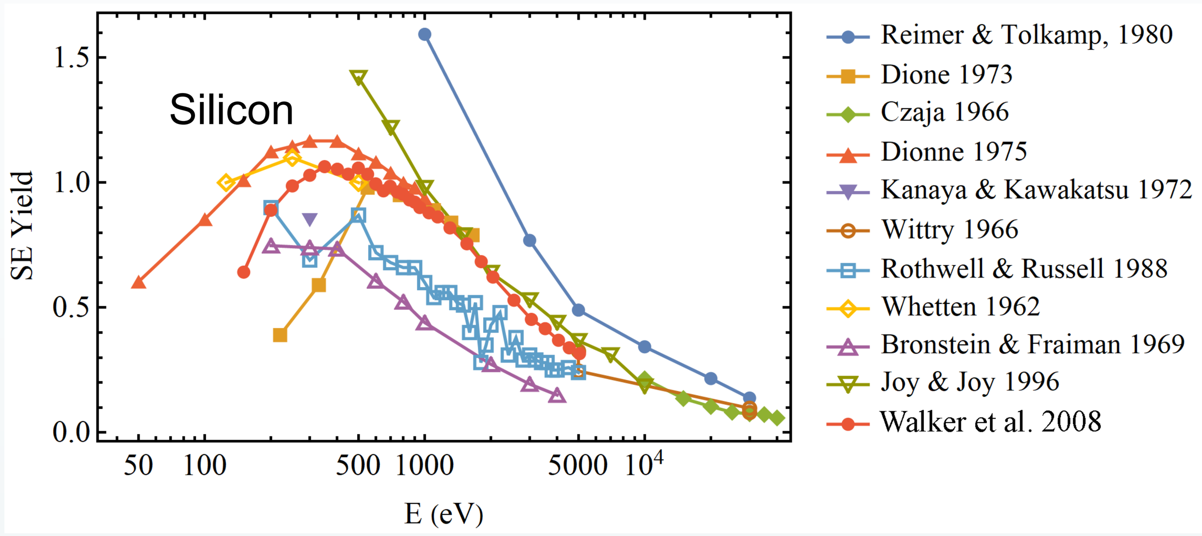


There is considerable scatter in the measurements and very little existing data for yield vs. angle of incidence, rendering such measurements a blunt instrument for distinguishing among models.

The scatter may be due to differences in surface cleanliness or disorder.

## Our Model Validation Approach

We are constructing an ultra-high vacuum (UHV) system with cleaning capabilities in a sample-prep chamber (left of the gate valve) and a spherical retarding field analyzer (RFA) in a measurement chamber (right).

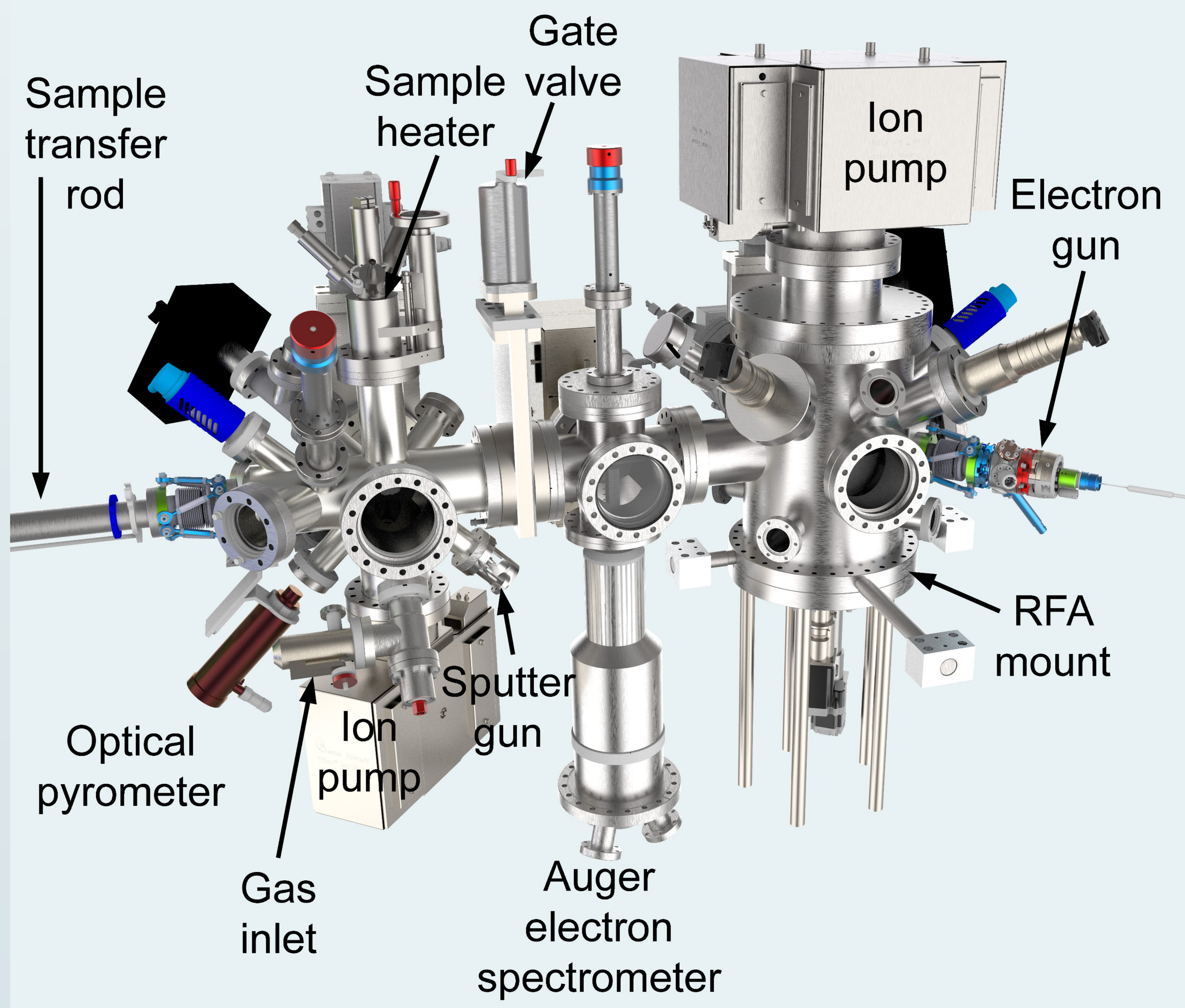


Sample cleaning capabilities will include:
- Neon and argon sputter-ion cleaning
- Sample heating (to anneal surface damage)
- Reactive gases, hydrogen or oxygen, to remove reactive contaminants from a heated sample
- Ultra-high vacuum to maintain cleanliness
- Electron irradiation cleaning
- Residual gas analyzer to characterize vacuum

Sample cleanliness characterization will be by Auger electron spectroscopy in the measurement chamber.

Spherical retarding field analyzer (RFA)

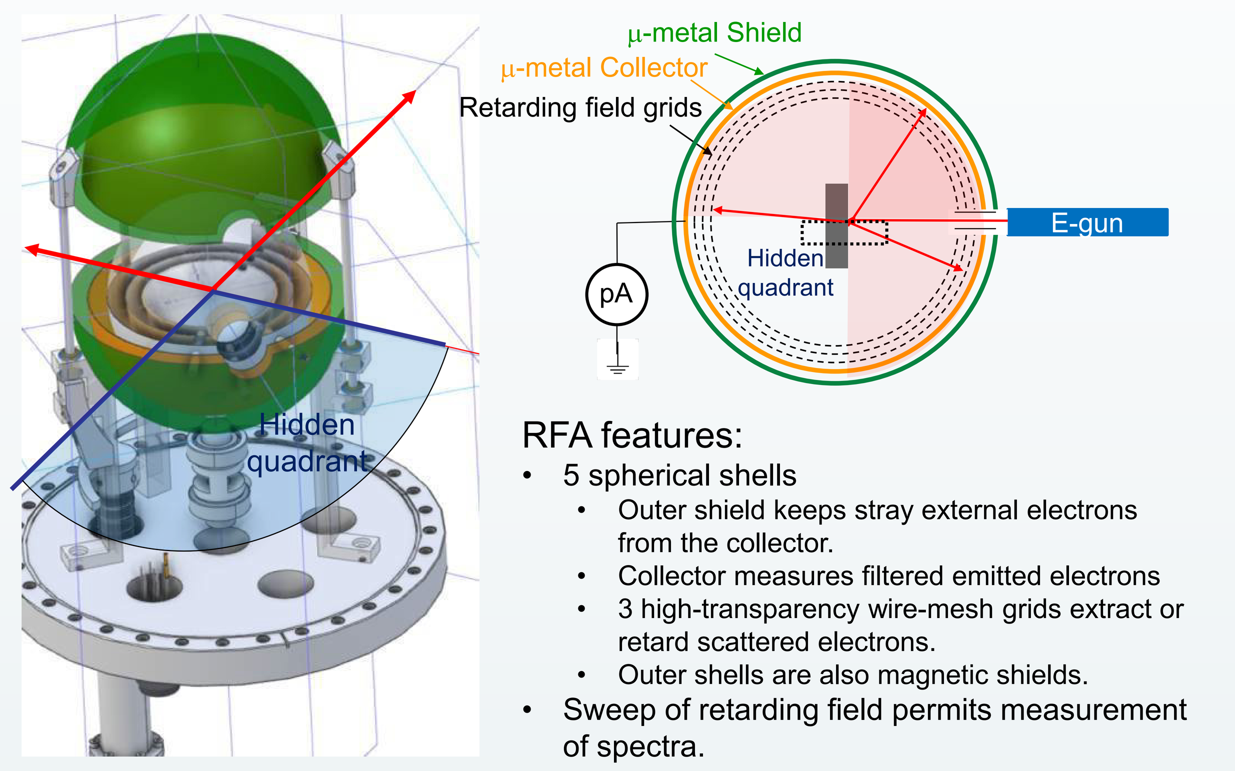


RFA features:
- 5 spherical shells
  - Outer shield keeps stray external electrons from the collector.
  - Collector measures filtered emitted electrons
  - 3 high-transparency wire-mesh grids extract or retard scattered electrons.
  - Outer shells are also magnetic shields.
- Sweep of retarding field permits measurement of spectra.

- Sample rotates to permit measurements vs. incident angle, θ.
- As θ varies from 0° to 90°, scattered electrons are collected in 3 quadrants (shaded)
- The hidden quadrant will be used for sample transfer and grid support, leaving the rest of the analyzer nearly invariant with angle for constant collection efficiency.
- Collector, sample, and grids will be independently biased and the currents independently measured.

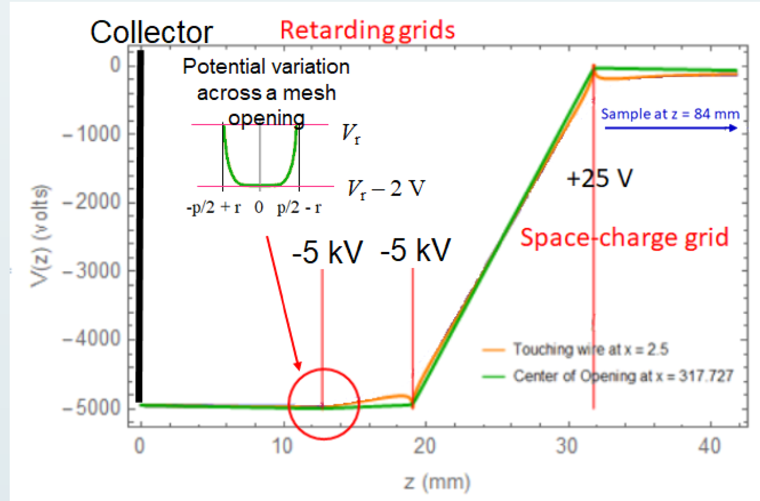


Calculated potential vs. position in the RFA in the most extreme condition: maximum retarding field. Resolution and shift of spectral peaks depends on potential uniformity (shown inset) across the grid in the circled region.

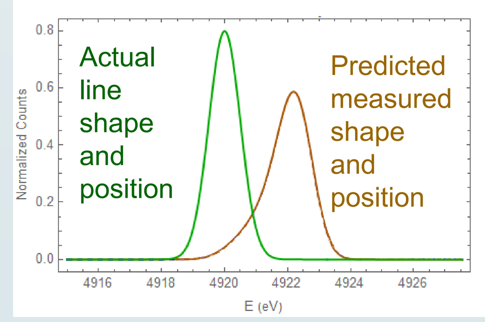


Expected resolution (change in line shape) and shift of peaks (0.2%) in the most extreme condition, based on a method of images calculation. (Actual performance should be about a factor of 2 better than this, because the calculation omits half the lines from the grid to preserve the symmetry required for this kind of calculation.)

## Summary

- Dimensional uncertainty in SEM is dominated by model uncertainty.
- Different models make widely divergent predictions of mean free paths and yields at electron energies below ~200 eV.
- A paucity of accurate and consistent measurement data render model selection difficult.
- This poster describes a new measurement system under construction. It will use state of the art cleaning and sample characterization and be able to measure:
  - Absolute electron yields vs. energy
  - Absolute electron yields vs. angle of incidence
  - Energy spectra of emitted electrons
- Such measurements will be reference data useful to validate electron transport models, thereby improving SEM metrology.

## References


1. J.S. Villarrubia et al., Ultramicroscopy 154 (2015) 15-28
2. A. Jablonski, F. Salvat, and C.J. Powell, J. Phys. Chem. Ref. Data 22 (2004) 409.
3. D.R. Penn, Phys. Rev. B 35 (1987) 482-486.
4. J. Llacer and E.L. Garwin, J. Appl. Phys. 40 (1969) 2766.
5. J.P. Ganachaud and A. Mokrani, Surf. Sci. 334 (1995) 329.
6. N.D. Mermin, Phys. Rev. B 1 (1970) 2362.